OPEN

Dual-Energy Computed Tomography Virtual Noncalcium Technique in Diagnosing Osteoporosis: Correlation With Quantitative Computed Tomography

Zhenghua Liu, MM, Yuting Zhang, MM,* Zhou Liu, MD,† Jiangtao Kong, MM,* Dageng Huang, PhD,‡ Xiaoyue Zhang, PhD,§ and Yonghong Jiang, MD**

Objective: The aim of this study was to evaluate dual-energy computed tomography (CT) virtual noncalcium (VNCa) technique as a means of quantifying osteoporosis.

Methods: Dual-energy CT scans were obtained prospectively, targeting lumbar regions of 55 patients with chronic low back pain. A standard quantitative CT (QCT) phantom was positioned at the waist during each procedure, using proprietary software (QCT Pro; Mindways, Tex) to measure bone mineral density (BMD) in each vertebral body. Vendor dual-energy analytic software was altered with a specially modified configuration file to produce a "Virtual Non Calcium" or "VNCa" output, as such output variables were remapped to produce the following calcium values rather than iodine, yielding the following QCT parameters: CT value of calcium (originally "contrast media" [CM]), CT value of mixed energy imaging (regular CT value [rCT]), calcium density (originally "contrast agent density" [CaD]), and fat fraction (FF). Pearson test served to assess correlations between BMD and these parameters. Multiple linear regression analysis was applied to construct an equation for generating regressive BMD (rBMD) values. In gauging diagnostic accuracies, the criterion-standard BMD cutoff point (<80 mg/cm^3) was adopted for QCT, whereas the rBMD threshold was defined by receiver operating characteristic curve.

Results: Contrast media, rCT, CaD, and FF values (reflecting CT value of calcium, regular CT value, calcium density, and fat fraction, respectively) significantly correlated with BMD (r values: 0.885, 0.947, 0.877, and 0.492, respectively; all $P < 0.01$). Contrast media, CaD, and FF showed independent associations with BMD; the regressive equation was formulated as follows: rBMD = 54.82 − 0.19 × CM + 20.03 × CaD − 1.24 × FF. The area under the curve of rBMD in diagnosing osteoporosis was 0.966 ± 0.009 ($P < 0.01$). At an rBMD threshold of less than 81.94 mg/cm^3, sensitivity and specificity were 90.0% and 92.0%, respectively.

Conclusions: Dual-energy CT VNCa technique may constitute a valid alternative method for quantifying the mineral content and marrow fat composition of bone in diagnostic assessments of osteoporosis.

Key Words: bone density, computed tomography, dual-energy scanned projection, osteoporosis, radiography, x-ray

(*J Comput Assist Tomogr* 2021;45: 452–457)

Osteoporosis (OP) is generally characterized as a skeletal disorder of reduced bone strength that heightens the risk of fracture. Bone mineral density (BMD) determinations are thus very important in this condition for both early diagnosis and therapeutic monitoring.[1,2] At present, dual x-ray absorptiometry (DXA) and quantitative computed tomography (QCT) are the 2 methods most widely used for this purpose in clinical and scientific research.[3,4]

Although DXA is officially cited as the preferred method,[5] some studies have cast doubt on its diagnostic accuracy in early OP. Dual x-ray absorptiometry is a projection-based technology that does not distinguish between trabecular and cortical BMD and may be influenced by adjacent calcific vascular walls.[6] In early diagnostic and curative assessments of OP, QCT-based determinations of BMD are considered superior to those of DXA.[7] Quantitative CT is a 3-dimensional process capable of distinguishing between cortical and cancellous bone and separately measuring trabecular densities.[8,9]

It has been shown that bone marrow fat is critical in BMD readings, increasingly skewing values lower as fat content rises.[10–12] Some sources have even linked higher fat content to occurrences of fracture in fragile vertebrae, suggesting its use as an independent index of such events.[11,13] Although the fat content of marrow clearly impacts BMD values, undermining vertebral strength, and is a needed parameter in research related to senile OP, it cannot be assessed by way of single-energy QCT. The large uncertainty in the fat content of marrow and the variability in distribution of fat make dual-energy approaches necessary for accurate determinations of vertebral mineral density.[14]

Dual-energy CT (DECT) is a rapidly growing tool in musculoskeletal radiology. In conjunction with virtual noncalcium (VNCa) technique, DECT can be used for quantitative analysis of specific substances, such as iron, calcium, and fat.[10,15,16] Some attempts at BMD measurement by DECT, particularly those involving phantom and cadaver experiments, have helped to underscore its considerable potential in quantifying vertebral body BMD,[17–21] whereas some indicate a lack of correlation between DECT-based volumetric BMD and areal BMD of DXA.[17,18]

It was our expectation that calcium and fat quantification by DECT VNCa technique might reveal a point-to-point correlation with QCT-based BMD values. Consequently, we studied the relations between specific calcium and fat markers quantified by DECT and QCT-measured BMD, establishing a mathematical regression model.

From the *Department of Radiology, Xi'an Jiaotong University Affiliated Honghui Hospital; †Department of Radiology, Xi'an International Medical Center Hospital; ‡Department of Spinal Surgery, Xi'an Jiaotong University Affiliated Honghui Hospital; and §Siemens Healthcare Limited, Xi'an, China.

Received for publication November 19, 2020; accepted February 13, 2021.

Correspondence to: Yonghong Jiang, MD, Department of Radiology, Xi'an Jiaotong University Affiliated Honghui Hospital, No. 555, Youyi East Road, Xi'an 710054, China (e-mail: 526017009@qq.com).

This study was funded by Innovative Talents Promotion Program (2020kjxx-023) and Shaanxi Provincial Key Research and Development Program (2020gxlh-y-027).

The authors of this article declare relationships with Siemens R&D Center Xi'an. Coauthors from Siemens have provided some scientific and technical support for this study. They had no access to and were not involved in the collection or analysis of the data in this study.

DOI: 10.1097/RCT.0000000000001168

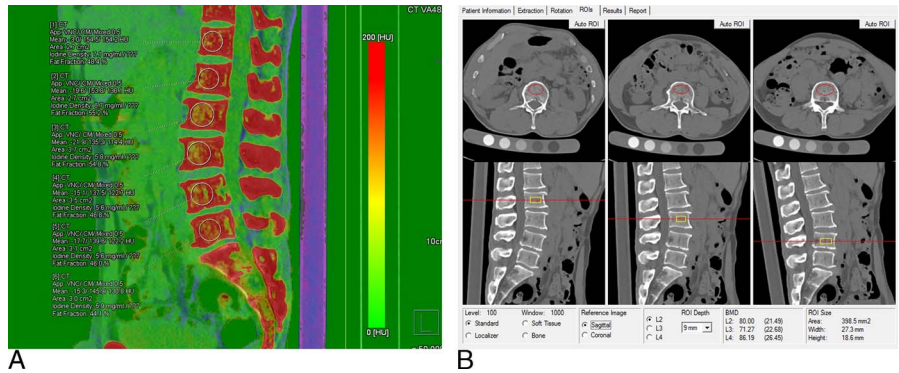

FIGURE 1. Quantitative osteoporotic parameters of DECT and QCT: (A) CM, rCT, CaD, and FF derived from corresponding ROI (DECT VNCa technique); (B) BMD determined by ROI drawn in front of the vertebral body (QCT Pro system). Note that because of modifications to the vendors, VNC software is to provide results for calcium instead of iodine.

Our intent was to explore a new DECT method for quantitative evaluation of OP, based on mineral content and marrow fat composition.

MATERIALS AND METHODS

Study Design

The present study adopted a forward-looking design, which the ethics committee of our hospital approved. With the informed consent of each participant, DECT scanning of lumbar regions was undertaken during March 2019 in patients with chronic low back pain. The scans were deemed necessary and advised by spinal surgeons at our facility, selecting subjects at random. By placing a standard corrected phantom beneath the scanning mattress, we obtained DECT parameters and QCT-based BMD determinations concurrently for each vertebral body. Thus, no additional radiation exposure was entailed.

All images were read by a senior physician with 15 years of experience in spinal CT. Localized osteosclerosis (n = 5), fracture (n = 3), neoplasm (n = 2), or postoperative change (n = 2) in any vertebral body was grounds for exclusion from this analysis.

CT Scanning

All CT examinations relied on a second-generation 128-section dual-source unit operating in dual-energy mode (Somatom Definition Flash; Siemens Healthineers, Erlangen, Germany). A standard QCT phantom (QCT Pro v5.0; Mindways, Tex) was placed at waist level during sessions. Settings of both x-ray tubes were constant (tube A: 80 kV, 250 mAs; tube B: 140 kV with Sn filter, 97 mAs). Scanning parameters were as follows: rotation time, 0.5 seconds; temporal resolution, 290 milliseconds; and pitch, 0.6. Scanning range extended from the upper edge of the 12th thoracic vertebral body to the lower edge of the first sacral vertebral body. Images were reconstructed using a kernel of I30f, a section thickness of 1 mm, and an increment of 0.75 mm. All radiation doses received by patients were recorded upon completion.

DECT Quantification of Calcium and Fat Parameters

Referring to the bone marrow configuration file of dual-energy analytic software (Syngo.via VB10; Siemens Healthcare, Erlangen, Germany), the default parameters in the liver virtual noncontrast (VNC) configuration file were modified, in order to quantify calcium and fat,[16,22] revising default values of soft tissue to 55 and 51 Hounsfield units (HU), assigning fat values (−110 and −87 HU) to yellow bone marrow, and substituting a calcium slope of 1.71 for the default iodine slope. In this way, the quantitative parameters of the liver VNC, the CT value for contrast media (CM) and the contrast agent density (CaD), correspond to the CT value for calcium and the calcium density in this experiment, respectively. By adjusting multiplanar reformation images to achieve a standard median sagittal plane, a round region of interest (ROI) was delineated in two-thirds of the anterior vertebral body, avoiding vertebral vein sulcus and surrounding areas of bony sclerosis (Fig. 1A). The CT value for calcium (CM), CT value of mixed- energy imaging (regular CT value [rCT]), calcium density (CaD), and fat fraction (FF) were measured for each vertebral body.

BMD Measured by QCT

Computed tomography equipment and QCT analytics (Mindways Software) were calibrated in advance using a quality control phantom. Computed tomography scan data of mixed ratio (0.5) were imported to the QCT software application. The BMD of each vertebral body was measured within an ROI encompassing two-thirds of the anterior vertebral body (Fig. 1B). All vertebral bodies were designated OP or non-OP, according to QCT-based BMD values, taking BMD of less than 80 mg/cm^3 as the diagnostic standard.[23]

TABLE 1. Statistics of Patients (n = 55)

	Age, y	High, cm	Weight, kg	BMI, kg/m^2	CTDI, mGy	DLP, mGy * cm
Mean (SD)	49.8 ± 12.1	161.48 ± 33.65	61.35 ± 18.21	23.40 ± 4.16	9.53	332.36 ± 40.26
Scope	25–77	150–176	45–84	17.6–30.6	9.53	230–435

BMI indicates body mass index; CTDI, CT dose index; DLP, dose-length product.

TABLE 2. Statistics of Vertebral Bodies (n = 318)

Group	BMD, mg/cm^3	CM, HU	rCT, HU	CaD, mg/cm^3	FF, %
OP (n = 87)	58.78 ± 15.14	128.77 ± 24.55	93.52 ± 25.33	5.15 ± 1.04	57.99 ± 10.67
Non-OP (n = 231)	128.44 ± 32.15	200.64 ± 40.62	180.94 ± 46.45	8.20 ± 1.78	48.69 ± 13.23
t	19.403	15.466	16.637	15.040	−5.877
P	0.000	0.000	0.000	0.000	0.000

Because of modifications to the vendors, VNC software is to provide results for calcium instead of iodine.

Statistical Analysis

All vertebrae measurements were performed by 2 experienced doctors. The consistency analyses were performed by intraclass correlation coefficient, and the mean value was taken as the final value. All computations were powered by standard software (SPSS v22.0; IBM, Armonk, NY), expressing data as means ± SDs. Variables were tested for normality of distribution by Shapiro-Wilk test, evaluating those with normal distribution via paired *t* test. Pearson test was applied to determine correlations between BMD and individual DECT parameters (CM, rCT, CaD, or FF), and a mathematical model of multiple linear regressions was established through regression analysis. Diagnostic accuracy of the mathematical model was determined by receiver operating characteristic curve, incorporating the QCT criterion-standard for BMD (<80 mg/cm^3).[23] Significance was set at $P < 0.05$ indicated for all tests.

RESULTS

A total of 318 vertebral bodies were evaluated in 55 patients, including 29 men and 26 women. Physical conditions of these patients and the radiation doses received are shown in Table 1. The

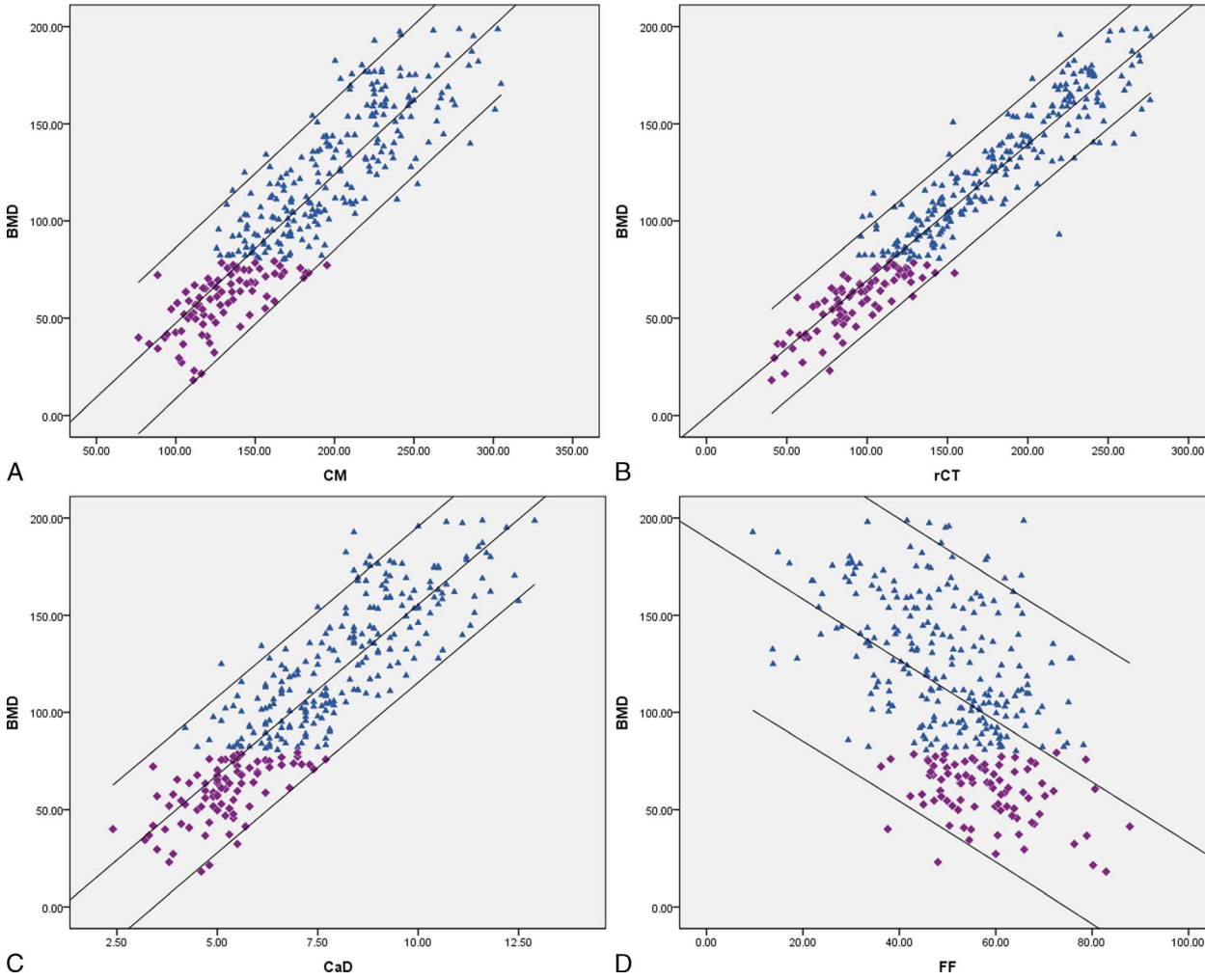

FIGURE 2. Correlation of BMD with CM, rCT, CaD, and FF: (A–C) significant positive correlations of CM ($r = 0.885$, $P < 0.01$), rCT ($r = 0.947$, $P < 0.01$), and CaD ($r = 0.877$, $P < 0.01$) with BMD and (D) significant negative correlation of FF with BMD ($r = 0.492$, $P < 0.01$). Because of modifications to the vendors, VNC software is to provide results for calcium instead of iodine.

TABLE 3. Multivariate Linear Regression Analysis of BMD

Model	*B*	β	*t*	*P*
(Constant)	54.823		7.476	0.000
CM	−0.190	−0.221	−2.281	0.023
rCT	0.029	0.039	0.252	0.801
CaD	20.031	1.005	7.110	0.000
FF	−1.240	−.389	−7.151	0.000

Because of modifications to the vendors, VNC software is to provide results for calcium instead of iodine.

QCT BMD values and DECT parameters (CM, rCT, CaD, or FF) measured by the 2 doctors were in good agreement, and the intraclass correlation coefficients were 0.990, 0.934, 0.951, 0.968, and 0.914, respectively (all $P < 0.01$). All vertebral bodies were designated OP or non-OP, and the 2 groups differed significantly in terms of BMD, CM, rCT, CaD, and FF values (Table 2).

Correlation/Regression Analyses

Pearson test showed significant correlation between BMD and CM, rCT, CaD, or FF ($r = 0.885$, 0.947, 0.877, and 0.492, respectively; all $P < 0.01$) (Fig. 2). By multiple linear regression analysis, CM, CaD, and FF were included in the regression equation, and the determinant coefficient was 0.915 (Table 3). The formula for generating regressive BMD (rBMD) values was as follows: $\text{rBMD} = 54.82 - 0.19 \times \text{CM} + 20.03 \times \text{CaD} - 1.24 \times \text{FF}$.

Diagnostic Accuracy

The receiver operating characteristic curve demonstrated better diagnostic accuracy for rBMD than for CM, CAD, or FF in this context (Fig. 3). The area under the curve of rBMD in diagnosing OP was 0.966 ± 0.009 ($P < 0.01$). At an rBMD threshold of less than 81.94 mg/cm^3, high degrees of sensitivity (90.0%) and specificity (92.0%) were observed.

DISCUSSION

We used VNCa technology in our research. Because the CT value of calcium substance is significantly higher than that of yellow bone marrow and red bone marrow, the lines from pure calcium to yellow bone marrow and from pure calcium to red bone marrow can be approximately regarded as 2 parallel straight lines, and the slope is the characteristic value of calcium.[16,22] According to this characteristic value, the CT value of calcium at any point on the CT value two-dimensional map and the CT value after virtual calcium removal can be calculated, so as to realize the quantitative measurement or removal of calcium content. In our study, a modification of the liver VNC configuration file was served in dual-energy analytic software, in order to quantify calcium and fat, using CM, rCT, CaD, and FF as chief parameters, which was different from the quantitative method of calcium and fat in previous studies.[10,14,17] In this way, the quantitative parameters of the liver VNC, CM, and CaD correspond to the CT value of calcium related and the CaD in this experiment, respectively, which are key components of BMD. Fat fraction also impacts BMD determinations, representing the content ratio of yellow bone marrow. In this study, CM and CaD positively correlated with QCT-based BMD values, whereas FF expectedly showed a negative correlation with BMD. Contrast media, CaD, and FF (all included in our regression equation) displayed high degrees of fitting. Receiver operating characteristic curve analysis further attested to the high diagnostic accuracy achieved, given the BMD regression equation our model provided.

Region-of-interest location appears critical in relating CT-based vertebral bone measurements and fracture.[24] Herein, ROI was confined

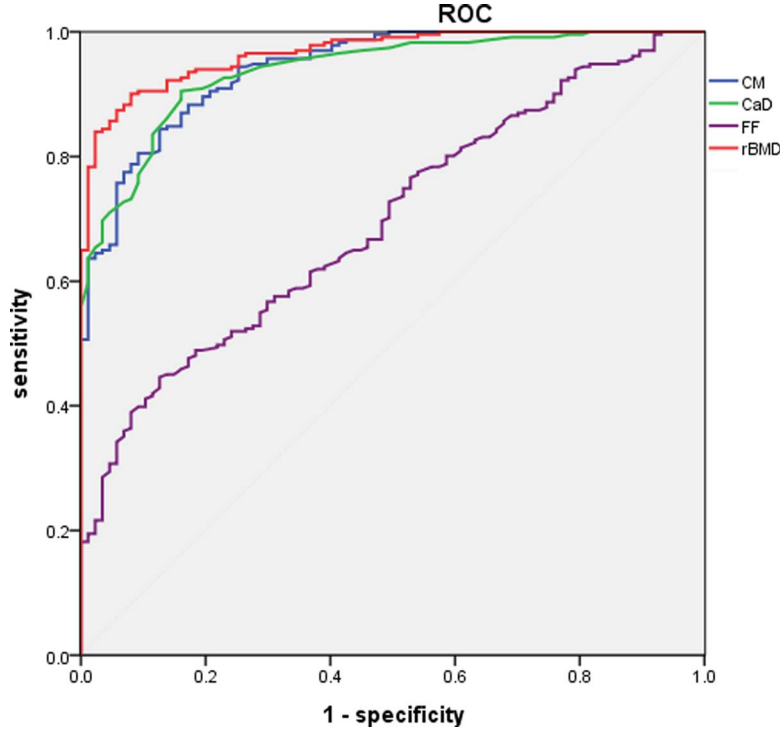

FIGURE 3. Receiver operating characteristic curve of CM, CaD, FF, and rBMD (areas under the curve, 0.941, 0.938, 0.696, and 0.966, respectively). Note that because of modifications to the vendors, VNC software is to provide results for calcium instead of iodine.

to the anterior two-thirds area of the vertebral body for 2 reasons: (1) to effectively avoid ossification of the vertebral vein groove and its margin and thus reduce BMD measurement error and (2) to focus on the area of concentrated stress prone to osteoporotic fracture, which is the anterior column.[25] Such emphasis has been lacking in previous studies, the entire vertebral body serving as ROI in certain instances.[17,26] These are unfortunate lapses, failing to fully exploit 3-dimensional technologic assets, although reliance on DXA as control method may have created an impediment. However, we did our best to ensure point-to-point correspondence of ROI and avoid system errors, regardless of methodology (DECT or QCT).

For the present investigation, we used a CT system with 2 simultaneously operating x-ray tubes. Dual-layer spectral detector CT has been similarly applied by others to assess BMD.[20,26–28] Both approaches share the same working principle, namely, a decomposition algorithm of dual-energy sources for differentiating various materials, although horizontal comparison has yet to be done. We used DECT VNCa technology to our advantage in quantifying calcium and fat content of vertebral bodies, injecting several meaningful parameters more inclined to accurately depict OP; and VNCa proved useful in evaluating bone marrow edema.[29–32] Ultimately, our method enabled quantitation of OP and bone marrow edema in the course of conventional CT diagnosis, as a one-stop examination scheme, helping reduce radiation exposures in part.

There are limitations to this study that merit discussion. Relevant research suggests that there is at present no accurate measure of bone strength, and BMD is a surrogate marker, accounting for ~70% of bone strength.[2] In addition to aging and lifestyle effects, manifested as intensified oxidative stress and glycosylation, nonenzymatic cross-linking of molecular collagen within the bony matrix may also undermine skeletal integrity.[33] Bone mineral density and fat content are thus merely indirect measures of bone strength, regardless of which is invoked. In the latest research, scholars have studied the relationship between OP and bone marrow fat and proposed a method to detect the risk of OP-related fractures using PET/CT data.[34] Thus, actual bone strength and fracture risk assessment are our objective in DECT assessments of OP; further investigation is clearly warranted.

At this juncture, the chief advancement is a 1-stop concept for elderly patients with OP, whereby a single CT scan suffices to diagnose vertebral fracture, check for marrow edema (indicative of fresh fracture), and assess OP. The entire process is then optimized, shortening treatment time, reducing costs, and lowering radiation risk.

CONCLUSIONS

Quantitative parameters for calcium and fat measured by DECT VNCa technique correlate significantly with QCT-based BMD determinations. Dual-energy CT VNCa technique is a valid means to quantitatively evaluate OP through bone mineral content and marrow fat quantitation.

REFERENCES

1. Siris ES, Adler R, Bilezikian J, et al. The clinical diagnosis of osteoporosis: a position statement from the National Bone Health Alliance Working Group. *Osteoporos Int*. 2014;25:1439–1443.
2. NA. NIH Consensus Development Panel on Osteoporosis Prevention, Diagnosis, and Therapy, March 7–29, 2000: highlights of the conference. *South Med J*. 2001;94:569–573.
3. Link TM. Osteoporosis imaging: state of the art and advanced imaging. *Radiology*. 2012;263:3–17.
4. Shepherd JA, Schousboe JT, Broy SB, et al. Executive summary of the 2015 ISCD position development conference on advanced measures from DXA and QCT: fracture prediction beyond BMD. *J Clin Densitom*. 2015; 18:274–286.
5. Morse LR, Biering-Soerensen F, Carbone LD, et al. Bone mineral density testing in spinal cord injury: 2019 ISCD official position. *J Clin Densitom*. 2019;22:554–566.
6. Bolotin HH. DXA in vivo BMD methodology: an erroneous and misleading research and clinical gauge of bone mineral status, bone fragility, and bone remodelling. *Bone*. 2007;41:138–154.
7. Loffler MT, Jacob A, Valentinitsch A, et al. Improved prediction of incident vertebral fractures using opportunistic QCT compared to DXA. *Eur Radiol*. 2019;29:4980–4989.
8. Engelke K, Adams JE, Armbrecht G, et al. Clinical use of quantitative computed tomography and peripheral quantitative computed tomography in the management of osteoporosis in adults: the 2007 ISCD Official Positions. *J Clin Densitom*. 2008;11:123–162.
9. Luo Y, Yang H. Comparison of femur stiffness measured from DXA and QCT for assessment of hip fracture risk. *J Bone Miner Metab*. 2019;37: 342–350.
10. Bredella MA, Daley SM, Kalra MK, et al. Marrow adipose tissue quantification of the lumbar spine by using dual-energy CT and single-voxel ^{1}H MR spectroscopy: a feasibility study. *Radiology*. 2015;277: 230–250.
11. Schellinger D, Lin CS, Lim J, et al. Bone marrow fat and bone mineral density on proton MR spectroscopy and dual-energy x-ray absorptiometry: their ratio as a new indicator of bone weakening. *AJR Am J Roentgenol*. 2004;183:1761–1765.
12. Rosen CJ, Ackert-Bicknell C, Rodriguez JP, et al. Marrow fat and the bone microenvironment: developmental, functional, and pathological implications. *Crit Rev Eukaryot Gene Expr*. 2009;19:109–124.
13. Patsch JM, Li X, Baum T, et al. Bone marrow fat composition as a novel imaging biomarker in postmenopausal women with prevalent fragility fractures. *J Bone Miner Res*. 2013;28:1721–1728.
14. Laval-Jeantet AM, Roger B, Bouysee S, et al. Influence of vertebral fat content on quantitative CT density. *Radiology*. 1986;159:463–446.
15. Ai S, Qu M, Glazebrook KN, et al. Use of dual-energy CT and virtual non-calcium techniques to evaluate post-traumatic bone bruises in knees in the subacute setting. *Skeletal Radiol*. 2014;43:1289–1295.
16. Fischer MA, Reiner CS, Raptis D, et al. Quantification of liver iron content with CT-added value of dual-energy. *Eur Radiol*. 2011;21:1727–1732.
17. Wichmann JL, Booz C, Wesarg S, et al. Dual-energy CT–based phantomless in vivo three-dimensional bone mineral density assessment of the lumbar spine. *Radiology*. 2014;271:778–784.
18. Booz C, Hofmann PC, Sedlmair M, et al. Evaluation of bone mineral density of the lumbar spine using a novel phantomless dual-energy CT post-processing algorithm in comparison with dual-energy x-ray absorptiometry. *Eur Radiol Exp*. 2017;1:11.
19. Wichmann JL, Booz C, Wesarg S, et al. Quantitative dual-energy CT for phantomless evaluation of cancellous bone mineral density of the vertebral pedicle: correlation with pedicle screw pull-out strength. *Eur Radiol*. 2015; 25:1714–1720.
20. Wesarg S, Kirschner M, Becker M, et al. Dual-energy CT–based assessment of the trabecular bone in vertebrae. *Methods Inf Med*. 2012;51: 398–405.
21. van Hamersvelt RW, Schilham AMR, Engelke K, et al. Accuracy of bone mineral density quantification using dual-layer spectral detector CT: a phantom study. *Eur Radiol*. 2017;27:4351–4359.
22. Wu H, Zhang G, Shi L, et al. Axial spondyloarthritis: dual-energy virtual noncalcium CT in the detection of bone marrow edema in the sacroiliac joints. *Radiology*. 2019;290:157–164.
23. Ward RJ, Roberts CC, Bencardino JT, et al. ACR Appropriateness Criteria (R) osteoporosis and bone mineral density. *J Am Coll Radiol*. 2017;14: 189–202.

24. Anderson DE, Demissie S, Allaire BT, et al. The associations between QCT-based vertebral bone measurements and prevalent vertebral fractures depend on the spinal locations of both bone measurement and fracture. *Osteoporos Int*. 2013;25:559–566.

25. Pollintine P, Dolan P, Tobias J, et al. Intervertebral disc degeneration can lead to "stress-shielding" of the anterior vertebral body: a cause of osteoporotic vertebral fracture? *Spine (Phila Pa 1976)*. 2004;29:774–782.

26. Laugerette A, Schwaiger BJ, Brown K, et al. DXA-equivalent quantification of bone mineral density using dual-layer spectral CT scout scans. *Eur Radiol*. 2019;29:4624–4634.

27. Roski F, Hammel J, Mei K, et al. Bone mineral density measurements derived from dual-layer spectral CT enable opportunistic screening for osteoporosis. *Eur Radiol*. 2019;29:6355–6363.

28. Mei K, Kopp FK, Bippus R, et al. Is multidetector CT-based bone mineral density and quantitative bone microstructure assessment at the spine still feasible using ultra-low tube current and sparse sampling? *Eur Radiol*. 2017;27:5261–5271.

29. Wong WD, Shah S, Murray N, et al. Advanced musculoskeletal applications of dual-energy computed tomography. *Radiol Clin North Am*. 2018;56:587–600.

30. Nicolaou S, Liang T, Murphy DT, et al. Dual-energy CT: a promising new technique for assessment of the musculoskeletal system. *AJR Am J Roentgenol*. 2012;199:78–86.

31. Yang P, Wu G, Chang X. Diagnostic accuracy of dual-energy computed tomography in bone marrow edema with vertebral compression fractures: a meta-analysis. *Eur J Radiol*. 2018;99:124–129.

32. Li M, Qu Y, Song B. Meta-analysis of dual-energy computed tomography virtual non-calcium imaging to detect bone marrow edema. *Eur J Radiol*. 2017;95:124–129.

33. Karampinos DC, Ruschke S, Dieckmeyer M, et al. Quantitative MRI and spectroscopy of bone marrow. *J Magn Reson Imaging*. 2018;47:332–353.

34. Kay FU, Ho V, Dosunmu EB, et al. Quantitative CT detects undiagnosed low bone mineral density in oncologic patients imaged with ^{18}F-FDG PET/CT. *Clin Nucl Med*. 2021;46:8–15.